Fuzzy C-Means-Based Filtering of Airborne Lidar Data: A Grid Based Method

Salah, M.[1] and Trinder, J.[2]
[1]Department of Surveying Engineering, Faculty of Engineering Shoubra - Benha University , 108 Shoubra st., Cairo – Egypt, E-mail: engmod2000@yahoo.com
[2]School of Civil and Environmental Engineering, The University of New South Wales, UNSW Sydney NSW 2052 – Australia, E-mail: j.trinder@unsw.edu.au

Abstract
This study introduces a method for filtering lidar data based on Fuzzy C-Mean (FCM) clustering. This method is composed of four key steps. In the first step, a Digital Surface Model (DSM) is generated for the first and last pulses. In the second step, the generated DSM and the lidar intensity image are reshaped and applied as input data for a FCM clustering process to automatically classify buildings, trees, roads and ground. In the third step, The DSM pixels which correspond to roads and ground in the classified image are interpolated into a grid DTM while the pixels which correspond to buildings and trees are omitted from the interpolation process. Finally, the interpolated DTM is smoothed by a low-pass filter to remove low vegetation and other objects which might be classified as ground. Datasets from mountainous and flat urbanized areas were selected to test the proposed filter. To meet the objectives, the generated DTM was compared against reference data that was generated manually and both omission and commission errors were calculated. Experimental results suggest that, compared with the widely applied progressive TIN (triangular irregular network) densification (PTD), the FCM approach is able to reduce omission, commission and total errors by 7.06%, 7.17% and 5.26% respectively in the case of urbanized area, and by 4.25%, 2.02% and 1.81% respectively in the case of mountainous areas.

1. Introduction and Related Works

Airborne Light Detection and Ranging (lidar), also termed Airborne Laser Scanning (ALS) has become a reliable technique for data collection of the earth's surface. Because of its characteristics which include acquisition of first and last pulses, narrow field angles, and independence of shadows and object texture, it is considered as the most effective technique for the production of high resolution Digital Terrain Models (DTMs) (Gianfranco and Carla, 2007). In addition to height information, lidar systems also record the intensity, sometimes referred to as the amplitude, of each received echo. The intensity represents the reflectance characteristics of the surface in the near infrared spectra. Lidar intensity is an important information source and increases with the reflectivity of the target and decreases with the distance between sensor and the target (Langford et al., 2006). Nowadays the focus of lidar data processing has been on the development of algorithms to extract DTMs from the 3D point cloud (Zhang and Lin, 2013). In most ALS applications, filtering is a necessary step (Meng et al., 2010). Filtering is the process of separating on-terrain points (DTM) from points falling onto objects such as buildings, cars, trees, and other natural and human made objects. Sithole and Vosselman (2004) separated existing filtering methods into four classes: slope-based, surface-based, clustering/segmentation, and block-minimum algorithms. Among them, the first three classes of filtering methods are more popular. In slope-based approaches, if the slope is above a certain threshold then the highest point is assumed to belong to an off-terrain object. Vosselman (2000) pioneered the work on slope-based filtering. Some extensions of slope-based filters focus on the shape of structure elements (Sithole and Vosselman, 2003), the determination of adaptive slope parameters (Susaki, 2012) and topological analysis to remove very large buildings (Liu et al., 2013). The slope-based methods usually work well when object and terrain points are equally mixed. However, typical filter errors are encountered when this requirement is not met. In surface-based approaches, a parametric surface is created with a corresponding buffer zone above it which defines a region in 3D space where ground points are expected to reside (Sithole and Vosselman, 2004). Depending on the means of creating the surface, surface-based filtering methods can be further

divided into three subcategories: morphology-based filters (Zhang et al., 2003, Chen et al., 2008 and Li, 2013), iterative-interpolation-based filters (Kraus and Pfeifer, 1998, Briese et al., 2002 and Kobler et al., 2007) and progressive-densification-based filters (Axelsson, 2000 and Zhang and Lin, 2013). Surface-based approaches are preferred in engineering applications (Zhu and Toutin, 2013). Many morphological filters suffer difficulties in removing different sizes of objects with a fixed widow size. On the other hand, studies have reported limitations when trying to apply interpolation-based filters to surfaces with rough terrain and steep ground slope. As well, progressive-densification-based filters sometimes fail to detect the terrain points on break lines and step edges (Liu et al., 2013). Segment-based filters generally consist of two steps, the first one being segmentation and the second one being filtering based on the generated segments. Lohmann (2002) applied the compactness of these segments and the height difference to the neighboring segments in order to detect different types of areas. Lee (2004) first obtained planar patches from the points with a region growing method, and then these patches were grouped into a set of surface clusters. It was assumed that the connected and continuous surface patches belong to the same object. Sithole and Vosselman (2005) compared the neighboring segment heights in different directions and using a predefined set of rule search, segment was classified as object or ground. Shen et al., (2012) assumed that the ground segments are horizontal and lower than adjacent object segments. Segment-based filters are typically designed for urban areas where many step edges can be found in the data. Lin and Zhang (2014) proposed a segmentation-based filtering (SBF) method that is composed of three key steps: point cloud segmentation, multiple echoes analysis, and iterative judgment. A detailed review of the available approaches for lidar data filtering is given by (Meng et al., 2010). Sithole and Vosselman (2005) demonstrated that for non-complex landscapes most of the algorithms performed well, while for complex landscapes surface based filters performed better. They suggested using clustering and data fusion for filtering of complex urban landscapes. Clustering is a process of putting similar data into groups such that the similarity within a group is larger than among the groups. Clustering can be classified as: Soft Clustering (Overlapping Clustering) and Hard Clustering (Exclusive Clustering). In the case of soft clustering techniques, fuzzy sets are used to cluster data so that each point may belong to two or more clusters with different degrees of membership, between 0 and 1. On the contrary, in hard clustering techniques, data are grouped exclusively, so that if certain data belong to a specific cluster then it cannot be included in another cluster. In many situations, fuzzy clustering is more natural than hard clustering. Fuzzy C-Mean (FCM) is the most representative fuzzy clustering algorithms since it is suitable for tasks dealing with overlapping clustering. In FCM clustering, a set of n data points are given in a two-dimensional space and an integer c (the number of clusters) and the problem is to determine a set of n points in the given space called 'centers', so as to minimize the mean squared distance from each data point to its nearest center (Bora and Gupta, 2014). On the other hand, there have been relatively few applications of FCM in the field of remote sensing. Pan et al., (2004) proposed a FCM method of extraction of trees on a color aerial image using a set of texture and color features. Ameri et al. (2008) developed a semi-automatic road extraction system from multi-spectral and pan-sharpened IKONOS. Mostofi and Samadzadegan (2012) proposed a method for extracting buildings and roof shapes from irregular lidar data based on an adaptive FCM clustering method. To facilitate the separation of ground from non-ground points, using lidar heights and intensity information, which involves a significantly large volume of data with an irregular sampling pattern, a FCM-based approach has been proposed in this research. The goal is to integrate both data sources to increase the filtering accuracy, minimize computation time and reduce memory requirements. On the other hand, unlike most of the filtering algorithms, FCM needs no specified parameters such as building size, slope threshold, minimum edge length which should be determined based on experience and the complexity of the landscapes. This paper is organized in the subsequent sections as follows. Section 2 describes the study areas and data sources. Section 3 describes the experiments while Section 4 presents and evaluates the results. We summarize our results in Section 5.

2. Study Area and Data Sources

Test area 1 covers an approximate area of about 500x500m of the region surrounding the University of New South Wales (UNSW) campus, Sydney Australia. The area is a largely urban area that contains residential buildings, large campus buildings, a network of main roads as well as minor roads, trees, open areas and green areas, as shown and summarized in figure 1(a, b and c) and table (1) respectively. Test area 2 is a part of Bathurst city, NSW Australia. It is a largely rural area that contains small residential buildings, a network of roads, trees and green areas. First and last pulse lidar data was acquired over the area including the

lidar intensity data. The color (red, green and blue) images were captured by a Leica ADS40 line scanner sensor and supplied as an ortho image as shown in figure 1(d, e and f) and table (1).

3. Methodology

This study proposes a method for filtering airborne lidar data based on Fuzzy C-Mean (FCM) clustering. This method is composed of four key steps as shown in table (2). The four main procedures in lidar-based DEM generation are fully discussed in the following sections.

Table 1: Characteristics of image and lidar data sets.

Test area	Size	lidar Data		Aerial images	
		Sensor	wavelength	bands	pixel size
UNSW	0.5 x 0.5Km	Optech ALTM 1225	1.047μm	RGB	10cm
Bathurst	1 x 1Km	Leica ALS50	1.064 μm	RGB	50cm

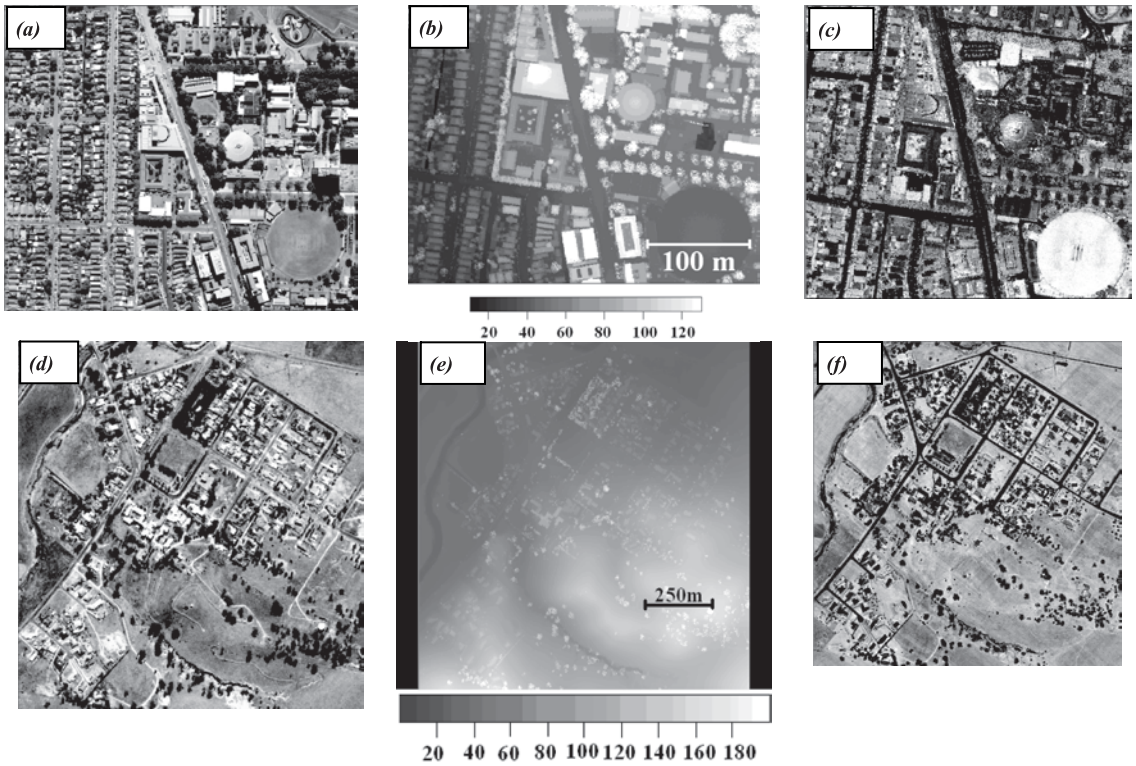

Figure 1:The selected study areas: (a), (b) and (c) are ortho image, DSM and lidar intensity of UNSW test area; (d), (e) and (f) are ortho image, DSM and lidar intensity of Bathurst test area.

Table 2: Algorithm filtering the lidar data

Data pre-processing
1. Generate a Digital Surface Model (DSM) from lidar point clouds. 2. Apply Subtractive Clustering to obtain the number of clusters *c* for the given sets of data.
FCM clustering
1. Input: reshape DSM and intensity images into a two columns vector. 2. Select *c* objects from *n* pixels as initial cluster centers. 3. Form *c* clusters by assigning each object to its closest center. 4. Recomputed the center *V* of each cluster until centers do not change. 5. Classify each pixel into a combination of memberships of clusters μ_{ik}. 6. Output: a set of *c* clusters
Generation of the DTM
1. Generate an initial DTM by comparing the DSM against the clustered image. 2. Output: Generate a final DTM by low-pass filtering of the initial DTM.
Accuracy assessment
1. Quantitative check of errors 2. Qualitative check of errors

3.1 Data Pre-Processing

Most lidar systems only record a few (1-5) reflections per transmitted pulse, and provide the option to choose amongst the first, first and last, or all reflections. The first echo of the incoming signal is referred to as *first pulse* and the last echo as *last pulse*. These systems are referred to as *discrete-return systems*. Data from both the first and the last pulse echoes were used in order to obtain denser terrain data and hence a more accurate filtering process. For each pixel in the generated images, its digital number (DN) is equal to the Z value of the lidar point that falls into the calculated pixel. For pixels with no corresponding lidar point, an interpolation process from neighboring pixels is applied to avoid introducing new height values. If more than one point falls within the same pixel, the minimum value is assigned to that pixel. The raster DSM and intensity images were then resampled to 50 cm x 50 cm cell size by bilinear interpolation. For the implementation of FCM clustering, four land cover classes were identified for both datasets which are: buildings, roads, trees, grass. It is worth mentioning that the *Subtractive clustering* (Chi, 1994) has been applied to obtain a clear idea how many clusters there should be for the given sets of data. The subtractive clustering method assumes each data point is a potential cluster center and calculates a measure of the likelihood that each data point would define the cluster center, based on the density of surrounding data points. The algorithm first selects the data point with the highest potential to be the first cluster center. Then it removes all data points in the vicinity of the first cluster center according to predetermined radii, in order to determine the next data cluster and its center location. The variable `radii` is a vector of entries between 0 and 1 that specifies a cluster center's range of influence in each of the data dimensions, assuming the data fall within a unit hyperbox (range [0 1]). Small `radii` values generally result in finding a few large clusters. The best values for `radii` are usually between 0.2 and 0.5. In this work, a radius of 0.5 has been specified for all data dimensions. Finally, the algorithm iterates on this process until all of the data is within the `radius` of a cluster center. A detailed description of the subtractive clustering method is given by Chiu (1994).The cluster estimates obtained from the Subtractive clustering process has been used to initialize the iterative FCM. Before the FCM clustering could be performed, the raster DSM and intensity image had to be reshaped into a vector of two columns (DSM and the intensity image) and n_x * n_y rows where n_x and n_y are the dimensions of the data sets.

3.2 FCM Clustering

The clustering algorithm is performed with an iterative optimization of minimizing a fuzzy objective function (J_m) defined as Equation (1).

$$J_m = \sum_{i=1}^{c}\sum_{k=1}^{n}(\mu_{ik})^m d^2(x_k, V_i)$$

Equation 1

Where

c = number of clusters

n = number of pixels

μ_{ik}= membership value of i^{th} cluster of k^{th} pixel

m = fuzziness for each fuzzy membership.

x_k= vector of k^{th} pixel

V_i= center vector of i^{th} cluster

$d^2(x_k,V_i)$ = Euclidean distance between $x_k$and V_i

The membership (μ_{ik}) is estimated by the distance between k^{th} pixel and center of i^{th} cluster, and is constrained as follows:

$$\begin{cases} 0 \le \mu_{ik} \le 1 & \text{for all } i,k \\ \sum_{i=1}^{c} \mu_{ik} = 1 & \text{for all } k \\ 0 < \sum_{k=1}^{n} \mu_{ik} < n & \text{for all } i \end{cases}$$

Equation 2

The center of cluster (V_i) and the membership value (μ^{ik}) could be calculated by Equations (3) and (4), respectively.

$$V_i = \frac{\sum_{k=1}^{n}(\mu_{ik})^m x_k}{\sum_{k=1}^{n}(\mu_{ik})^m}, 1 \le i \le c$$

Equation 3

$$\mu_{ik} = \left[\sum_{j=1}^{c}\left(\frac{d(x_k,V_i)}{d(x_k,V_j)}\right)^{\frac{2}{m-1}}\right]^{-1}, 1 \le i \le c, 1 \le k \le n$$

Equation 4

Therefore, J_m can be minimized by iteration through Equations (3) and (4). The first step of the iteration is to initialize a fixed c, a fuzziness parameter (m), a threshold ε of convergence, and an initial center for each cluster, then computing μ_{ik} and V_i using Equations (3) and (4) respectively. The iteration is terminated when the change in V_i between two iterations is smaller than ε. Finally, each pixel is classified into a combination of memberships of clusters.

3.3 Generation of the DTM

An initial DTM was generated automatically by comparing the DSM against the classified image. All DSM pixels which correspond to roads or ground in the classified image were interpolated into a grid DTM and resampled to 1 m pixel size, while the pixels which correspond to buildings and trees were omitted from the interpolation process. The interpolated DTM was then low-pass filtered, to remove low vegetation and to compensate for the mis-classification errors at edges of buildings and trees.

3.4 Accuracy Assessment

In order to evaluate the performance of the proposed filtering method, the reference data was generated by manually filtering the lidar data sets with knowledge of the four landscapes and available aerial images. In this regard, the original lidar point clouds were overlaid on the ortho image and classified visually as either ground or non-ground features. The International Society for Photogrammetry and Remote Sensing (ISPRS) has followed this approach in order to provide a set of testing sites containing various ground elements and a set of classified ground truth data (Meng et al., 2010). Then, the FCM-based filtered lidar data was compared against the manually filtered data. There are two basic errors in filtering of lidar data. One is the classification of non-ground measurements as ground points or commission errors, and the other is the assignment of ground points as non-ground measurements or omission errors (Congalton, 1991). All filtering methods are subject to these two types of errors to various degrees. To evaluate the performance of filtering techniques, these errors should be examined as follows, based on the parameters in Table (3). The widely used PTD filtering method was also tested and compared to our proposed method. This method is widely employed in both the scientific community and engineering applications, because it has been integrated into the commercial software TerraSolid. TerraScan is the main application in the Terrasolid software family for managing and processing lidar point clouds. TerraScan enables the automatic filtering of the point cloud. The implementation of this method is as follows. The whole point dataset is first divided into tiles, and then the lowest points in each block is selected as the initial ground points, and a TIN of the identified ground points is constructed as the reference surface. For each triangle, one additional ground point is determined by investigating the parameters of the unclassified points in each triangle with the reference surface. The parameters are the distance to the TIN facets and the angles to the nodes. If a point is found with offsets below an experienced threshold values, 0.5m in this research, it is classified as a ground point and the algorithm proceeds with the next triangle. Before continuing with the next iteration, all ground points are added to the TIN. In this way, the triangulation was progressively densified until all points are classified as ground or non-ground (Zhang and Lin, 2013 and Sithole and Vosselman, 2004). All the methods proposed in this research were implemented through a software package generated by the authors in a Matlab environment under the Windows XP Operating System. The hardware used is a PC, with an Intel Pentium 1.86GHz CPU and 1.87 GB RAM.

4. Results and Discussion

In order to run the FCM algorithm, the parameters are set to the same values for the two datasets. The total number of clusters c is initialized as 4, maximum number of iteration as 100, exponent for μ_{ik} as 2.0 and a minimum improvement ε of 1^{e-6}. The clustering process stops when the maximum number of iterations is reached, or when the objective function improvement between two consecutive iterations is less than the minimum amount of improvement specified.

Table 3:Definition of omission and commission errors

	ground	**non-ground**	
ground	a	b (omission error)	e = a + b
non-ground	c (commission error)	d	f = c + d
	g = a + c	h = b + d	n = a + b + c + d

Percentage of omission errors: b / e * 100%
Percentage of commission errors: c / f *100%
Percentage of total errors: (b + c) / n * 100%

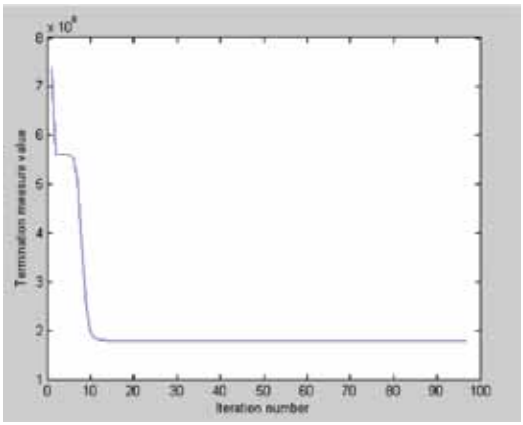

(a) Termination measure plot

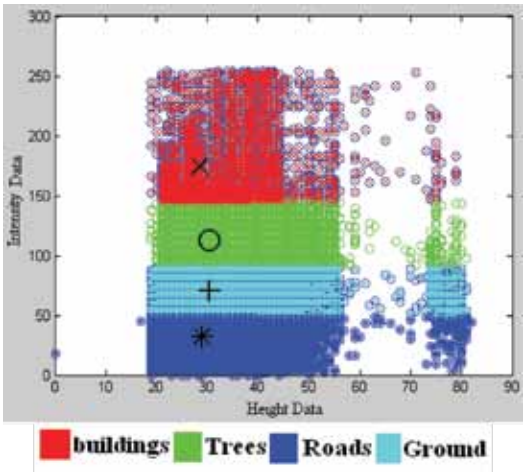

(b) Scattered Fuzzy C-Means graph with final fuzzy cluster centers

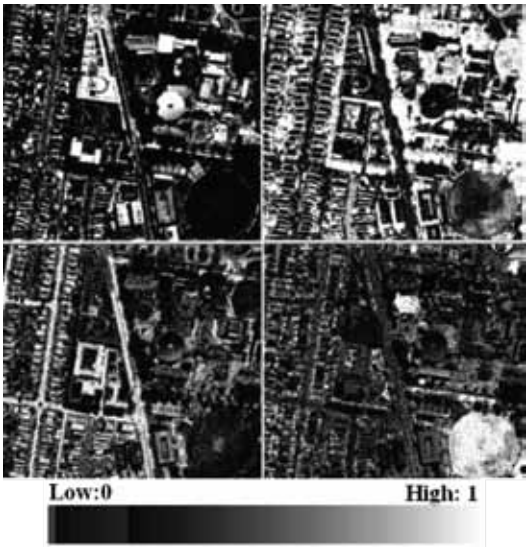

(c) Membership values of the FCM in the case of UNSW.

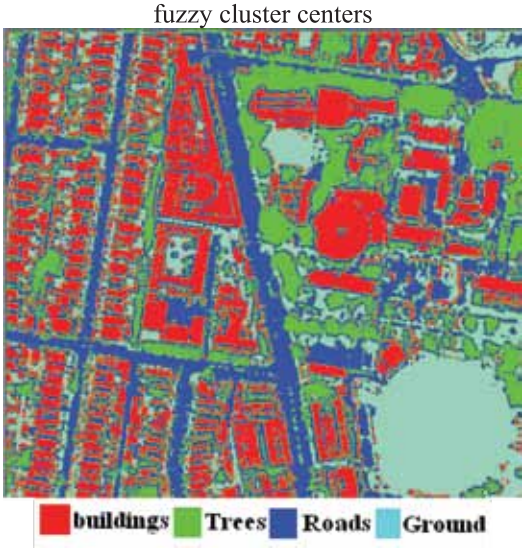

(d) Final FCM clustering results

(e) Ground pixels in black and non-ground pixels in white

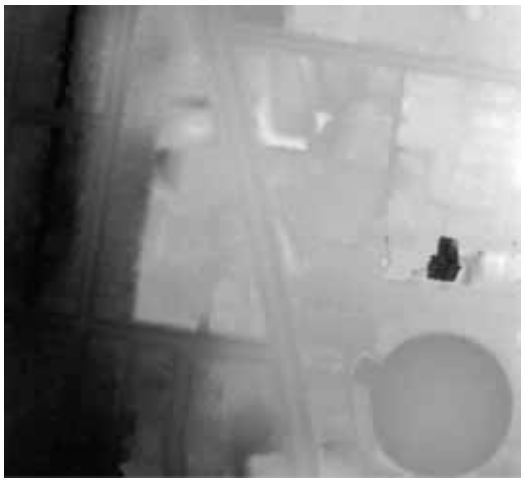

(f) Smoothed FCM-based DTM

Figure 2: The detailed steps for FCM filtering method in the case of Urbanized test area

4.1 Urbanized Area

For UNSW test area and at maximum iteration count = 97, the value of the objective function obtained is 178866515.384163 as shown in figure (2a). Data points of each cluster are displayed in different colors, while the clusters centers are displayed in black markers (o, x, * and +) as shown in figure (2b). Figure (2c) shows a typical example of the FCM output which is the decision values of each pixel for each class. The probability values represent true probability in the range of 0 to 1, and the sum of these values for each pixel equals 1. The probability values have been used later to create a new classification image, as shown in figure (2d), without having to recalculate the entire classification. The membership values from all the land covers were compared and the class with the highest membership value was assigned to the pixel label. Buildings and trees were separated by converting their digital number to one, while the digital numbers of ground pixels (roads and trees) were converted to zeros. The result is a binary image as shown in figure (2e). DSM pixels which correspond to roads and ground in the classified image are interpolated into a grid DTM while the pixels which correspond to buildings and trees are omitted from the interpolation process.

The interpolated DTM is then smoothed by a low-pass filter to remove low vegetation and other objects which might be classified as ground. The final output is a smoothed DTM as shown in figure (2f). In order to evaluate the performance of the adopted method for filtering of lidar data. The results were compared with the reference data. The two types of errors are calculated, namely, type I errors (omission errors), type II errors (commission errors), together with the total errors for the two filtering methods as listed in Table (4) and shown in figure (3). Compared with the PTD, the type I, type II and total errors of the FCM method are reduced by approximately7.06%, 7.17% and 5.26% respectively. The reduced error values means that most of the ground observations are correctly retained. On the other hand, the increased error values in the case of PTD filter method indicate that the filter partially fails to meet the ground measurements in the reference data. Large commission errors indicate that the filter fails to remove the lower parts of the objects and to preserve the ground measurements as shown in the square region in figure (3). This leads us to conclude that, the FCM method is better able to achieve correct filtering results when the PTD algorithm fails.

Table 4: Errors incurred for the FCM and PTD filtering methods in the case of urbanized test area

Type of error	FCM (%)	PTD (%)
I	6.22	13.28
II	7.26	14.43
Total	6.81	12.07

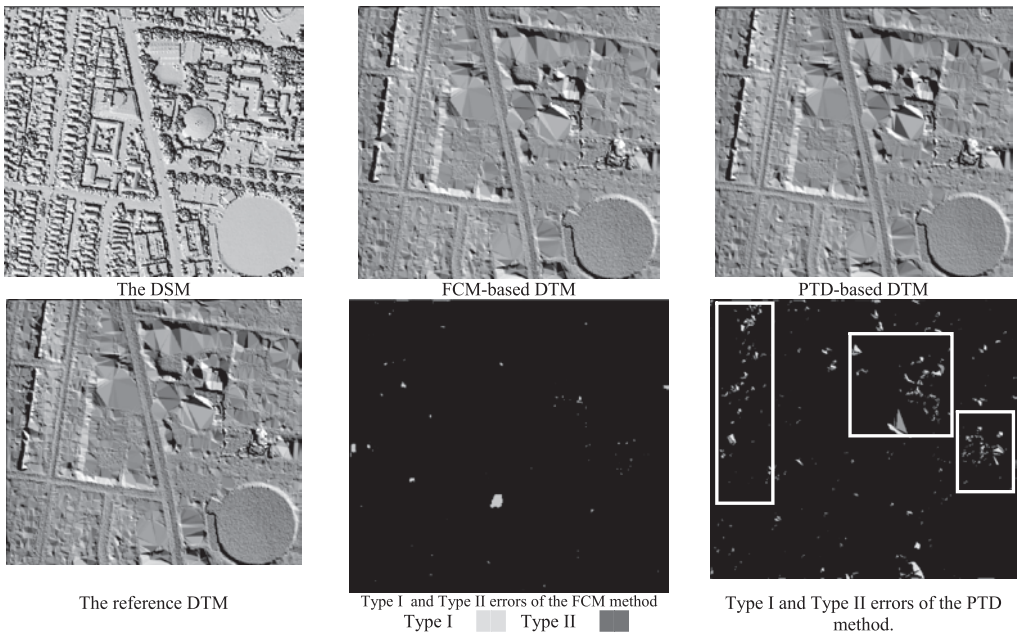

Figure 3: Filtering results of the urbanized test area

4.2 Rural Area

In the case of Bathurst test area, the parameters was set to the same values and the FCM algorithm was run. Figure (4) shows the detailed steps of the filtering process. Accuracy analysis of filtering results for the urban dataset, table (5), shows that both filters produced filtering accuracies comparable to each other. Compared with the PTD filter, the type I errors decrease from 6.52% to 2.27%, the type II errors decreased from 5.80% to 3.78%, and the total errors decrease from 5.09% to 3.28%.

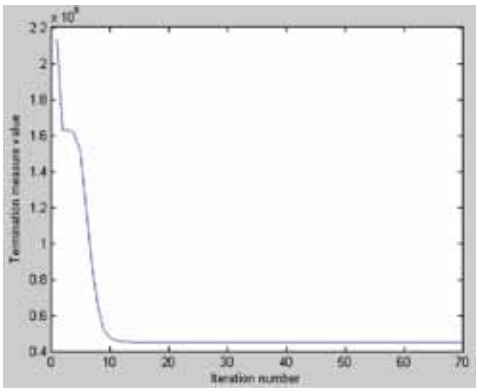

(a) Termination measure plot

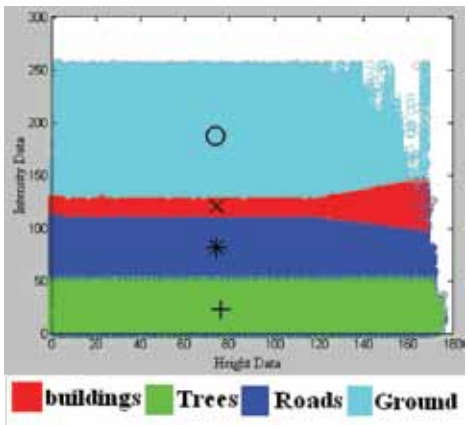

(b) Scattered FCM graph with final fuzzy cluster centers

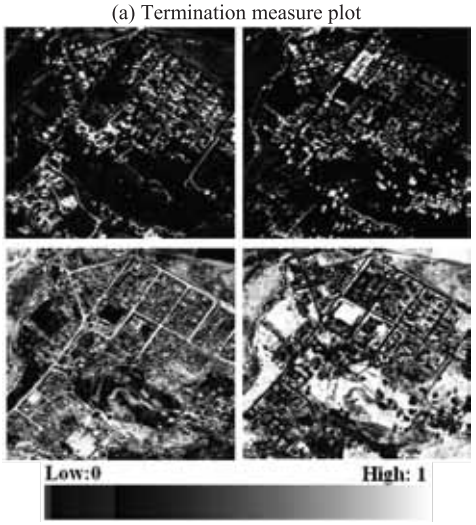

(c) Membership values of the FCM in the case of Bathurst.

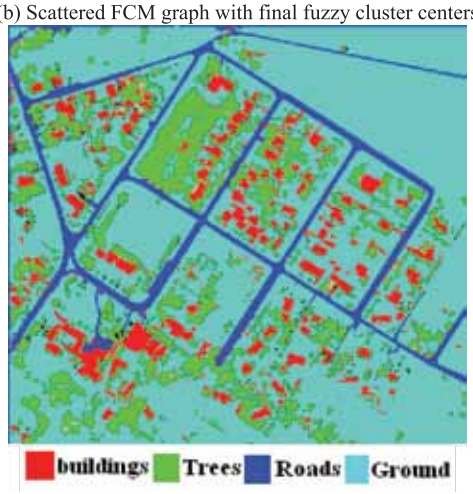

(d) Final FCM clustering results

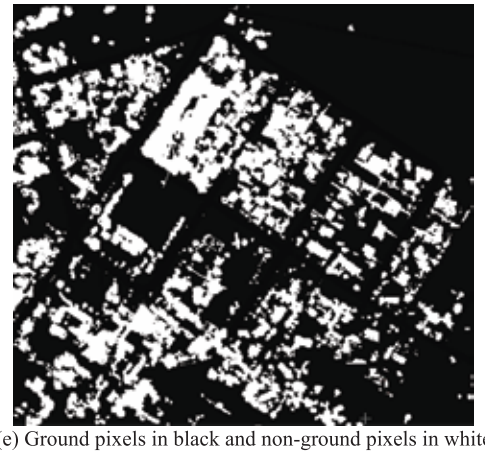

(e) Ground pixels in black and non-ground pixels in white

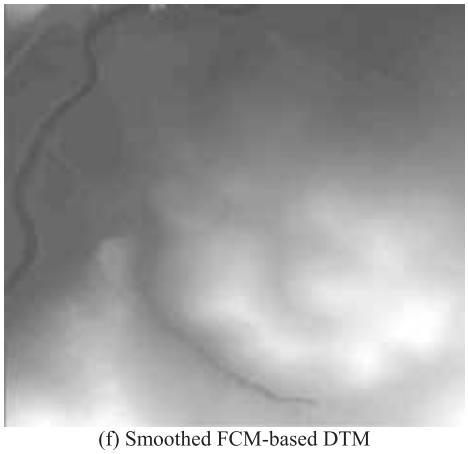

(f) Smoothed FCM-based DTM

Figure 4: The detailed steps for FCM filtering method in the case of Urbanized test area

Table 5: Errors incurred for the FCM and PTD filtering methods in the case of rural test area

Type of error	FCM (%)	PTD (%)
I	2.27	6.52
II	3.78	5.80
Total	3.28	5.09

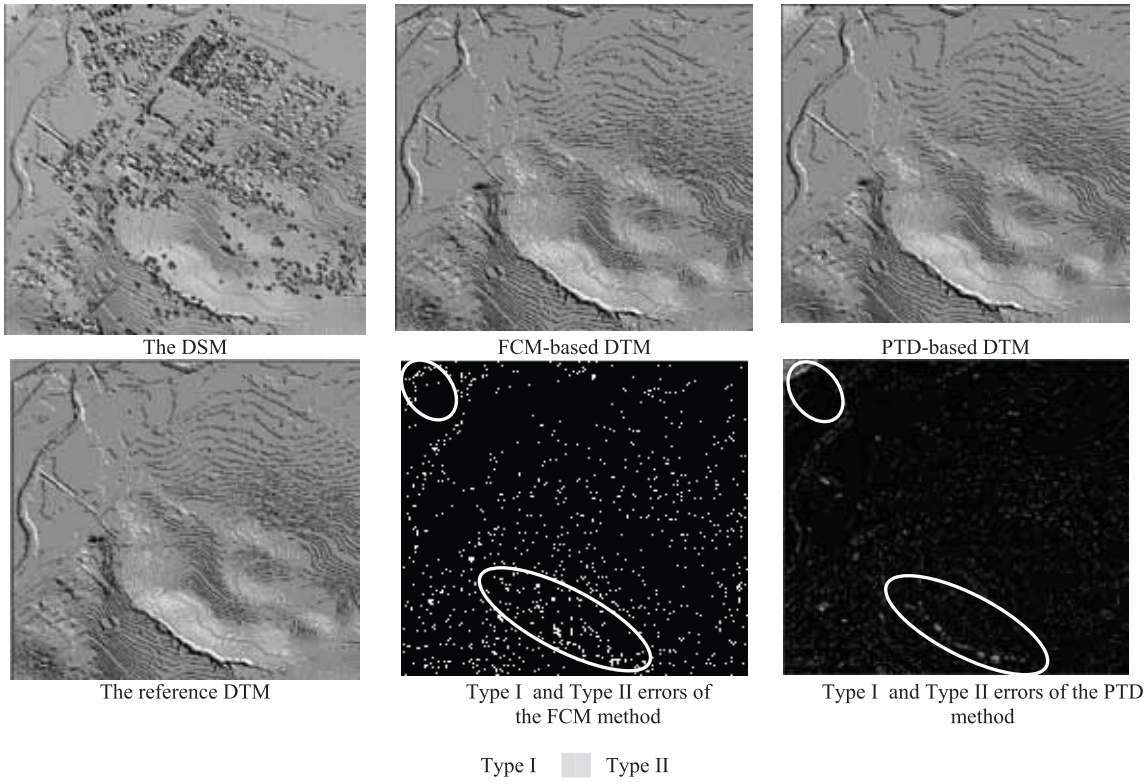

Figure 5: Filtering results of the rural test area

These results demonstrate the ability of FCM method to preserve ground measurements in areas with steep terrain. Another aspect of interests is that most errors occur at the ground points around discontinuity caused by natural break lines. A possible reason for this could be the effect of between-class variance on the edge pixels which caused many of these pixels to be placed in an incorrect category during the FCM clustering process. Figure (5) shows the error distribution map in case of the rural test area. It is worth mentioning that the PTD filtering method has failed to preserve ground measurements around the same steep areas when the FCM filter fails, as shown in the ellipse region in Figure (5).

5. Conclusions and Future Work

A method for filtering of lidar data based on the fusion of lidar and intensity data based on FCM clustering was presented. The algorithm is applied to the resampled lidar data to ensure that it is more rapid and efficient. The results suggest that the FCM approach is better than the widely used PTD filter in removing the non-ground measurements and preserving the ground measurements in both the urban and mountain areas accurately and effectively. In the case of urbanized area and as compared with the PTD filtering method, the errors were reduced by 7.06%, 7.17% and 5.26% for omission, commission and total errors respectively. In the case of rural area, the errors were reduced by 4.25%, 2.02% and 1.81% respectively. On the other hand, the filtering process is highly automatic and requires little human interference. Future research should be directed at the improvement of the proposed method based on multi-source data fusion. As well, this algorithm has to be tested in other datasets in different kinds of areas.

Acknowledgments
The authors would like to acknowledge AAMHatch for the provision of the UNSW datasets and the Department of Lands, NSW, Australia for Bathurst datasets.

References

Ameri, F., Mobaraki, A. and Valadan Zoej, M., 2008, Semi-Automatic Extraction of Different-Shaped Road Centerlines from MS and Pan-Sharped Ikonos Images. *International Archives of the Photogrammetry, Remote Sensing and Spatial Information Sciences*, 37, 621-626.

Axelsson, P., 2000, DEM Generation from Laser Scanner Data using Adaptive TIN Models. *International Archives of Photogrammetry and Remote Sensing*, 33, 203– 210.

Bora, D. J. and Gupta, A. K., 2014, A Comparative Study between Fuzzy Clustering Algorithm and Hard Clustering Algorithm. *International Journal of Computer Trends and Technology,* 10(2), 108-113.

Briese, C., Pfeifer, N. and Dorninger, P., 2002, Applications of the Robust Interpolation for DTM Determination. Int. Arch. Photogramm. *Remote Sensing*, 34, 55–61.

Chen, C. F., Chang, H. Y. and Chang, L. Y., 2008, A Fuzzy-Based Method for Remote Sensing Image Contrast Enhancement. *International Archives of the Photogrammetry, Remote Sensing and Spatial Information Sciences*. 37, 995- 1000.

Chiu, S., 1994, Fuzzy Model Identification Based on Cluster Estimation, *Journal of Intelligent and Fuzzy Systems*, 2(3), 267-278.

Congalton, R. G., 1991, A Review of Assessing the Accuracy of Classifications of Remotely Sensed Data. *Remote Sensing of Environment*, 37(1), 35–46.

Gianfranco, F. and Carla, N., 2007, Adaptive Filtering of Aerial Laser Scanning Data. *Proceedings of ISPRS Workshop on Laser Scanning 2007*, 12-14 September 2007, Espoo, Finland, 173-177.

Kobler, A., Pfeifer, N. and Ogrinc, P., Todorovski, L., Oštir, K. and Džeroski, S., 2007, Repetitive Interpolation: A Robust Algorithm for DTM Generation from Aerial Laser Scanner Data in Forested Terrain. *Remote Sensing of Environment*, 108(1), 9–23.

Kraus, K. and Pfeifer, N., 1998, Determination of Terrain Models in Wooded Areas with Airborne Laser Scanner Data. *ISPRS Journal of Photogrammetry and Remote Sensing*, 53(4), 193-203.

Langford, J., Niemann, O., Frazer, G., Wulder, M. and Nelson, T., 2006, Exploring Small Footprint Lidar Intensity Data in a Forested Environment. *Proceedings of IEEE International Conference on Geoscience and Remote Sensing Symposium*, 31 July - 4 August 2006, Denver, Colorado, 2416–2419.

Lee, I., 2004, A Feature Based Approach to Automatic Extraction of Ground Points for DTM Generation from Lidar Data. In Proceedings of the ASPRS Annual Conference, 23–28 May 2004, Denver, CO, USA.

Li, Y., 2013, Filtering Airborne Lidar Data by an Improved Morphological Method Based on Multi-Gradient Analysis. *International Archives of the Photogrammetry, Remote Sensing and Spatial Information Sciences*, XL-1/W1, 191-194.

Lin, X. G. and Zhang, J. X., 2014, Segmentation-Based Filtering of Airborne lidar Point Clouds by Progressive Densification of Terrain Segments. *Remote Sensing,* 6(2), 1294-1326; doi:10.3390/rs602129

Liu, J., Shen, J., Zhao, R. and Xu, S., 2013, Extraction of Individual Tree Crowns from Airborne Lidar Data in Human Settlements. *Mathematical and Computer Modelling*, 58, 524–535.

Lohmann, P., 2002, Segmentation and Filtering of Laser Scanner Digital Surface Models. *International Archives of the Photogrammetry, Remote Sensing and Spatial Information Sciences*, 34, 311–315.

Meng, X., Currit, N. and Zhao, K., 2010, Ground Filtering Algorithms for Airborne Lidar Data: A Review of Critical Issues. *Remote Sensing*, 6(2), 833–860.

Mostofi, N. and Samadzadegan, F., 2012, Segmentation of Lidar Data for Extracting Building's Roof Shapes, using Fuzzy Logic Concepts. *GIS Ostrava 2012 - Surface Models for Geosciences*, 23-25 January 2012, ostrava.

Pan, L., Zheng, H., Zhang, Z. and Zhang, J., 2004, A Height and Texture Information Integrated Approach for Object Extraction Applied to Automatic Aerial Triangulation. *International Archives of the Photogrammetry, Remote Sensing and Spatial Information Sciences*, 35, 382-386.

Shen, J., Liu, J. P., Lin, X. G. and Zhao, R., 2012, Object-Based Classification of Airborne Light Detection and Ranging Point Clouds in Human Settlements. *Sensor Letters*, 10, 221–229.

Sithole, G. and vosselman, G., 2003, Comparison of Filtering Algorithms. *Proceedings of the ISPRS working group WG III/3 workshop on 3-D reconstruction from airborne laserscanner and InSAR data- XXXIV-3/W13*, 8-10 October 2003, Dresden, Germany, 71–78.

Sithole, G. and Vosselman, G., 2004, Experimental Comparison of Filter Algorithms for Bare Earth Extraction from Airborne Laser Scanning Point Clouds. *ISPRS Journal of Photogrammetry and Remote Sensing*, 59, 85–101.

Sithole, G. and Vosselman, G., 2005, Filtering of Airborne Laser Scanner Data Based on Segmented Point Clouds. *International Archives of the Photogrammetry, Remote Sensing and Spatial Information Sciences*, 36, 66–71.

Susaki, J., 2012, Adaptive Slope Filtering of Airborne Lidar Data in Urban Areas for Digital Terrain Model (DTM) Generation. *Remote Sensing*, 4, 1804–1819.

Vosselman, G., 2000, Slope Based Filtering of Laser Altimetry Data. *International Archives of Photogrammetry and Remote Sensing*, 33(4), 958–964.

Zhang, J. X. and Lin, X. G., 2013, Filtering Airborne Lidar Data by Embedding Smoothness-Constrained Segmentation in Progressive TIN Densification. *ISPRS Journal of Photogrammetry and Remote Sensing*, 81, 44–59.

Zhang, K.Q., S.C. Chen, D. Whitman, M.L. Shyu, J.H. Yan, and C.C. Zhang, 2003, A Progressive Morphological Filter for Removing Non-ground Measurements From Airborne LIDAR Data. *IEEE Transactions on Geoscience and Remote Sensing*, 41 (4), 872–882.

Zhu, X. K. and Toutin, T., 2013, Land Cover Classification using Airborne Lidar Products in Beauport, Québec, Canada. *International Journal of Image and Data Fusion*, 4(3), 252–271.